Electron Transfer through H-bonded Peptide Assemblies

Heinz-Bernhard Kraatz,* Irene Bediako-Amoa, Samuel H. Gyepi-Garbrah, and Todd C. Sutherland

Department of Chemistry, University of Saskatchewan, 110 Science Place, Saskatoon, Saskatchewan, Canada S7N 5C9

Received: May 17, 2004; In Final Form: September 12, 2004

A series of ferrocene (Fc)- and cystamine (CSA)-labeled peptides of the sequence [Fc-(Pro-Pro-Gly)$_n$-CSA]$_2$, where $n = 1-3$, was synthesized and characterized. Peptide **3** forms a trimeric supramolecular structure held together with extensive hydrogen bonding and adopts a collagen-like motif in solution. Cyclic voltammetry (CV) and chronoamperometry (CA) were used to calculate electron-transfer (ET) kinetics. ET rates were 10.9 (2.3) $\times$ 10^3, 6.6 (1.9) $\times$ 10^3, and 4.2 (1.2) $\times$ 10^3 s^{-1} for peptides where $n = 1$, 2, and 3, respectively. The peptides, under deuterated conditions (D_2O, full exchange of H for D), showed rate constants of 7.3 (1.3) $\times$ 10^3, 5.8 (1.0) $\times$ 10^3, and 3.4 (0.5) $\times$ 10^3 s^{-1} for $n = 1$, 2, and 3, respectively. A linear dependence of the ET rate constant and distance is found.

Introduction

Understanding electron-transfer (ET) processes in proteins is of fundamental importance.[1−18] In a series of photophysical studies of well-behaved peptide model systems, it has become evident that the ET through the peptide spacer is greatly influenced by the separation between the acceptor (A) and the donor (D), the nature of the peptide backbone, the amino acid sequence, and the resulting flexibility.[18−21] In particular, it was suggested in the literature that the presence of H-bonding will increase the rate of ET, and there is experimental evidence (mostly in proteins) to suggest that H-bonding indeed increases the rate of ET.[3,22−28] Studies by Therien,[29] Nocera,[30−33] and Hamilton[34] on well-defined donor−acceptor systems, possessing a H-bonded linkage between the donor and the acceptor, have clearly demonstrated the importance of the H-bonded interface in influencing the ET process. Recently, a detailed study reported the influence of H-bonding on ET in α-aminoisobutyric acid (Aib) homooligomers having 3_{10}-helicity. In these systems, ET is influenced by the number of H-bonds in the peptide.[35] A Fc-glycine film that displays simple redox behavior, which has the potential for interstrand H-bonding, did not exhibit an influence of the ET kinetics on H-bonding.[36] A series of Fc-Gly-peptides with an increasing length of the Gly spacer displays an apparent change in the ET mechanism from a tunneling to a hopping mechanism.[36b] These results are supported by theoretical calculations on ET mechanisms carried out by Petrov and May.[72]

Electrochemical methods are ideal to investigate the ET and interfacial properties of an Fc-peptide film attached to an electrode surface.[37−40] In particular, cyclic voltammetry (CV), chronoamperometry (CA), and electrochemical impedance spectroscopy (EIS) are useful to obtain parameters, ranging from the footprint of electroactive molecules bound to a surface to the interfacial resistance exerted by the film to the ET kinetics.[41]

Here, we describe the results of an electrochemical study of ferrocenoyl (Fc)-labeled collagen-like peptides assembled onto a gold surface and provide evidence for H-bonding playing a role in the ET process in peptidic systems, which relates back to Gray's results on the importance of H-bonding in helical proteins.[3,22,25,27]

* Corresponding author. E-mail: kraatz@skyway.usask.ca.

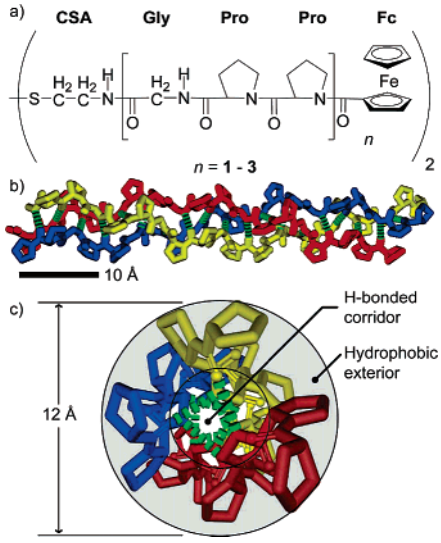

Figure 1. (a) Structure of compounds **1**−**3** studied. (b) Schematic of the supramolecular coiled-coil structure adopted by a Pro-Pro-Gly repeat unit taken from the solid-state structure.[50] (c) A view down the helical core showing the H-bonded corridor and the arrangement of the hydrophobic residue toward the exterior of the helical structure.

In contrast to earlier work on helical Fc-oligoprolines,[20] where the oligoprolines are unable to form intra- or interstand H-bonding patterns, the collagen-like peptides described here can engage in interstrand intermolecular H-bonding. For this reason, we have chosen the simple (Pro-Pro-Gly) repeat unit. Each single peptide strand adopts a left-handed polyproline-II structure. Three peptide strands assemble into a supramolecular right-handed triple helical structure by forming inter-peptide H-bonds between the amide NH of each glycine residue with the carbonyls of proline residues on adjacent peptide strands, as illustrated in Figure 1. The net results is that H-bonding occurs on the interior of the triple helix providing, for longer peptides, a H-bonded corridor on the interior with all aliphatic residues pointing toward the exterior of the triple helix.[42−50] Using these Fc-collagen conjugates, we hoped to address the following questions: Does interstrand H-bonding play a role in the ET mechanism? Is the H-bonded interface participating

10.1021/jp047900c CCC: $27.50
Published on Web 12/04/2004

in the ET? We expected that if a hopping mechanism involves hopping from amide to amide, as suggested by Kimura for α-helical systems,[11] a change of the conditions (deuteration, temperature) in a H-bonded system such as collagens should be measurable by electrochemical techniques. A collagen-like structure provides a well-defined framework to probe the role of H-bonded peptide assemblies in ET reactions. Currently, the mechanism of ET in H-bonded peptides is unclear. Surface ET studies may potentially clarify possible long-range ET mechanisms including tunneling, hopping, and even ion transport.

Experimental Section

General Procedure. All syntheses were carried out in air unless otherwise indicated. CH_2Cl_2 and $CHCl_3$ (BDH; ACS grade) used for synthesis, Fourier transform infrared spectroscopy (FT-IR), and electrochemistry were dried (CaH_2), and distilled under N_2 prior to use. Acetone, EtOAc, CH_3CN, MeOH, diethyl ether (BDH; ACS grade), hexanes (Fischer; HPLC grade), $CHCl_3$, and CH_2Cl_2 used for the purpose of purification were used as received. $CDCl_3$ and CD_3CN (Aldrich) were dried and stored over molecular sieves (8−12 mesh; 4 Å effective pore size; Fisher) before use. Acetone-d_6 (MSD) was used as received. EDC, HOBt, Boc-Pro-OH, H-Pro-OMe·HCl, H-Gly-OEt·HCl, Fc-COOH (Aldrich), $MgSO_4$, and $NaHCO_3$ (VWR) were used as received. Et_3N (BDH; ACS grade) used in Fc-amino acid couplings was dried over molecular sieves when used in stoichiometric quantities. For column chromatography, a column with a width of 2.7 cm (i.d.) and a length of 45 cm was packed 18−22 cm high with 230−400 mesh silica gel (VWR). For thin-layer chromatograpy (TLC), aluminum plates coated with silica gel 60 F_{254} (EM Science) were used. NMR spectra were recorded on a Bruker AMX-500 spectrometer operating at 500 (^{1}H) and 125 MHz (^{13}C{^{1}H}). Peak positions in both ^{1}H and ^{13}C spectra are reported in parts per million relative to TMS. ^{1}H NMR spectra of Fc-peptides are referenced to the CH_2Cl_2 resonance (δ 5.32 ppm) of an external standard ($CDCl_3/CH_2Cl_2$). ^{1}H spectra of all other compounds are referenced to the residual $CHCl_3$ signal. All ^{13}C{^{1}H} spectra are referenced to the $CDCl_3$ signal at δ 77.23 ppm.

Infrared (IR) and reflection absorption infrared (RAIR) spectra were recorded from a Bio-Rad FTS-40 system interfaced to a PC. Circular dichroism (CD) spectra were recorded with an Applied Photophysics π*-180 instrument interfaced to an Acorn PC. Mass spectra were run on a QSTAR XL-MS/MS system.

The synthetic procedures for the formation of the Fc-peptide conjugates **1**−**3** was achieved by coupling of ferrocene carboxylic acid with the corresponding peptide cystamine. The procedure is described in detail for compound **1**.

*[Fc-(Pro$_2$-Gly)-CSA]$_2$ (**1**):* [Boc-(Pro$_2$-Gly)-CSA]$_2$ (0.06 g, 0.095 mmol) was dissolved in trifluoroacetic acid (2 mL) at 0 °C in an ice bath. It was stirred at room temperature for 15 min. Then the mixture was evaporated, and the residue was dried by addition of benzene and evaporation repeated three times. The product was dissolved in CH_2Cl_2 (10 mL) and neutralized by Et_3N (0.02 mL, 0.11 mmol) at 0 °C in an ice bath to obtain the solution of H-(Pro$_2$-Gly)$_2$-CSA. To a solution of ferrocene monocarboxylic acid (0.018 g, 0.079 mmol) in 15 mL of CH_2Cl_2, hydroxybenzotriazole (HOBt) (0.017 g, 0.11 mmol) and 1-(3-dimethylaminopropyl)-3-ethylcarbodiimide (EDC) (0.021 g, 0.11 mmol) were added at 0 °C in an ice bath. The solution of [H-(Pro$_2$-Gly)$_2$-CSA]$_2$ was added after 30 min to the stirring reaction mixture of Fc(COOH), HOBt, and EDC in an ice bath. The resulting solution was washed by 15 mL of 10% citric acid, saturated $NaHCO_3$, and H_2O, respectively. The organic phase was dried over Na_2SO_4 and then evaporated to dryness. The crude product was purified by flash column chromatography (FCC) on silica gel, giving an orange solid (solvent CH_2Cl_2:MeOH = 98:2, R_F = 0.30, yield 67%). FT-IR (KBr disk): 1649, 1661 (br, C═O Pro and Gly). HRMS (FAB): calcd for $C_{50}H_{62}N_8O_8Fe_2S_2$ 1078.9080 [M$^+$]; found 1079.2914. ^{1}H NMR ($CDCl_3$): 8.43 (1H, m, NH), 7.32−7.13 (1H, m, NH), 4.79−3.67 (28H, m, Fc, αH, δH of Pro, αH of Gly), 2.73−2.46 (8H, m, CSA), 2.52−2.02 (16H, m, βH, γH Pro). ^{13}C{^{1}H} NMR ($CDCl_3$): 174.3, 173.1, 173.0, 172.6, 172.3, 172.2, 171.4, 171.2, 170.4, 170.3, 170.2, 170.1 (C═Pro and Gly), 77.7, 77.5, 77.2, 76.2 (tert C, Cp_{subst}), 71.6, 71.2, 70.9, 70.4 (CH, Cp_{subst}), 70.2, 70.0 (CH, $Cp_{unsubst}$), 61.4, 61.2, 60.1 (CH^{α} Pro), 49.1, 47.9, (CH_2^{β} CSA), 43.5, 43.4 (CH_2^{δ} Pro), 38.9, 38.2 (CH_2^{α} CSA), 29.2, 28.3 (CH_2^{β} Pro), 26.1, 25.9, 25.8, 25.7 (CH_2^{γ} Pro), 22.6, 19.3 (CH_2 Gly).

*[Fc-(Pro$_2$-Gly)$_2$-CSA]$_2$ (**2**):* FCC on silica gel (solvent CH_2Cl_2:MeOH = 12:1, R_F = 0.34, yield 70%). FT-IR (KBr disk) 1605, 1651 (br, C═O Pro and Gly). HRMS (FAB): calcd for $C_{74}H_{96}N_{14}O_{14}Fe_2S_2$ 1581.4882 [M$^+$]; found 1581.2914. ^{1}H NMR ($CDCl_3$): 8.43 (2H, m, NH), 7.32−7.13 (2H, m, NH), 4.79−3.67 (28H, m, Fc, αH, δH of Pro, αH of Gly), 2.73−2.46 (8H, m, CSA), 2.52−2.02 (16H, m, βH, γH Pro).^{13}C{^{1}H} NMR ($CDCl_3$): 172.2, 172.0, 171.5, 171.2, 170.9, 170.8, 169.7 168.7 (C═Pro and Gly), 79.6 (tert C, Cp_{subst}), 71.7, 71.6, 70.7 (CH, Cp_{subst}), 70.5, 70.1 (CH, $Cp_{unsubst}$), 615, 60.0, 59.5, 59.3, 58.5, 58.2 (CH^{α} Pro), 48.8, 47.8 (CH_2^{β} CSA), 47.5, 47.1 (CH_2^{δ} Pro), 39.3, 39.2, 38.4, 37.1 (CH_2^{α} CSA), 28.6, 28.2, 28.1, 28.0, (CH_2^{β} Pro), 26.1, 25.5, 25.2, 25.7 (CH_2^{γ} Pro), 22.5, 22.4 (CH_2 Gly).

*[Fc-(Pro$_2$-Gly)$_3$-CSA]$_2$ (**3**):* FCC on silica gel (solvent CH_2Cl_2:MeOH = 12:1, yield 69%, R_F = 0.28). FT-IR (KBr disk) 1607, 1649 (br, C═O Pro and Gly). HRMS (FAB): calcd for $C_{98}H_{130}N_{20}O_{20}Fe_2S_2$ 2084.0590 [M$^+$]; found 2084.2914. ^{1}H NMR ($CDCl_3$): 8.43 (2H, m, NH), 7.32−7.13 (2H, m, NH), 4.79−3.67 (28H, m, Fc, αH and δH of Pro, αH of Gly), 2.73−2.46 (8H, m, CSA), 2.52−2.02 (16H, m, βH, γH Pro).^{13}C{^{1}H} NMR ($CDCl_3$): 172.4, 172.2, 171.3, 171.2, 170.8, 171.1, 171.0, 170.7, 170.6, 170.2, 169.8, 169.8 (C═O Pro and Gly), 77.7, 77.4, 77.2 (tert C Cp_{subst}), 71.7, 70.7, (CH, Cp_{subst}), 70.6 70.1 (CH, $Cp_{unsubst}$), 61.4, 60.1, 59.6, 59.3, 58.3 (CH^{α} Pro), 49.0, 47.5, 47.4, 46.7 (CH_2^{β} CSA), 39.3−38.5 (CH_2^{δ} Pro), 28.7, 28.5, 28.2, 27.9 (CH_2^{β} Pro), 26.0, 25.3, 25.2 (CH_2^{γ} Pro), 22.5 (CH_2 Gly).

Preparation of Gold Microelectrodes. Gold wire (Alfa Aesar, 99.9%), 50 μm diameter, was fixed into a soft glass capillary tube by butane flame. The Au wire fixed into the soft glass was broken in half to expose the Au and then was polished with a 0.05 μm alumina slurry. Visual inspection of the electrode under a light microscope was done to ensure the glass−Au seal was intact. Additionally, the microscope was used to measure the geometric surface area as the Au wire melts while the glass seals, which can lead to diameters different from 50 μm. Electrical contact to the Au wire was made by Ag paste (Aldrich) to an Ag wire (0.1 mm diameter, Alfa Aesar, 99.9%). The Ag paste was dried for 24 h before fixing the silver wire to the glass tube with epoxy resin to provide mechanical stability. The electrode was electrochemically cycled from a potential of −0.1 to +1.25 V vs Ag/AgCl in 0.5 M H_2SO_4 solution until a stable gold oxidation peak at 1.1 V vs Ag/AgCl was observed. The surface roughness was evaluated by Cu UPD and was between 1.3 and 1.4.

Ellipsometry. Au on Si(100) (Platypus Technologies, Inc) wafers were incubated in a 1 mM Fc-peptide ethanolic solution for 5 days and finally rinsed with EtOH and H_2O. A Stokes ellipsometer LSE (Gaertner Scientific Corporation, Skokie, IL,

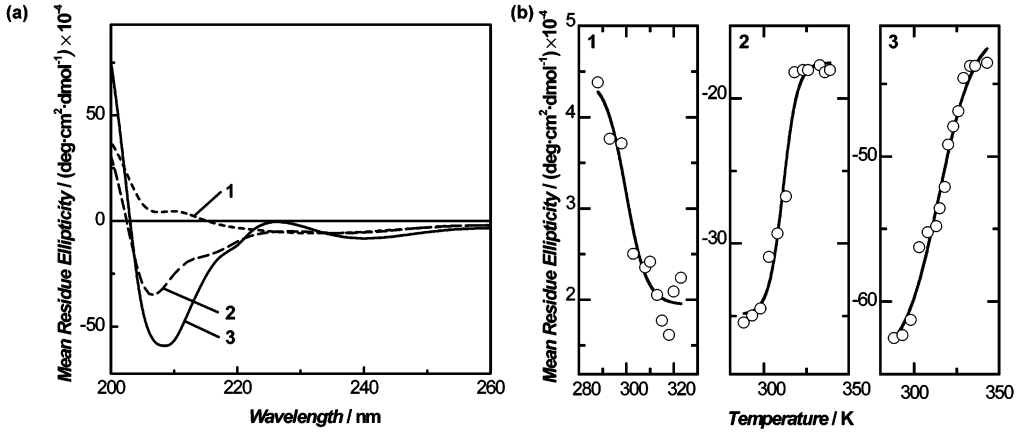

Figure 2. (a) CD spectra of compounds **1**−**3** at 15 °C in EtOH. (b) Melting curves of **1**−**3** obtained by monitoring the CD intensity at 209 nm.

fixed angle (70°), fixed wavelength (632.8 nm)) was used, and the data were collected and analyzed using LGEMP (Gaertner Ellipsometer Measurement Software) on a PC. Ellipsometry constants were as follows: $n_S = 0.25$ and $K_S = 3.46$ for the substrate and 1.40 was used as the refractive index of the monolayer.

Preparation of Fc-Peptide Modified Gold Electrodes. The gold microelectrodes or bulk polycrystalline gold electrodes (BAS) were incubated in 1 mM ethanolic solution of the Fc-peptides (**1**−**3**) for 5 days. The electrodes were rinsed with ethanol and then Millipore water (18.2 MΩ·cm) and finally sonicated for 120 s prior to any electrochemical experiment. The electrodes were then incubated in 1 mM ethanolic hexanethiol solution for 10 min to produce the mixed film. Deuterated modified gold electrodes were prepared by two methods. The first involved heating the 1 mM $CDCl_3$ solution (containing a drop of D_2O) of peptides **1**−**3** to 58 °C for 30 min. Full exchange of the hydrogen with deuterium was monitored by ^{1}H NMR of the amide region (see Supporting Information). Freshly cleaned gold electrodes were placed in the fully deuterated peptide solution that was cooled to room temperature in a sealed vial for 5 days. The electrodes were then sequentially rinsed with MeOD and D_2O and finally sonicated in D_2O for 120 s prior to electrochemical experiment. The second method is the same as the nondeuterated monolayer formation except it involved incubating the Fc-peptides (**1**−**3**) in EtOD for 5 days. These monolayers were rinsed consectively with EtOD and D_2O and then sonicated in D_2O for 120 s. Both methods to prepare deuterated monolayers resulted in the same isotope effect.

Cyclic Voltammetry (CV) Measurements. CV measurements were performed using a custom-built electrochemical system designed for microelectrodes. The gold microelectrode serves as a working electrode. The cell was enclosed in a grounded Faraday cage. A reference electrode was constructed by sealing Ag/AgCl wire into a glass tube with a solution of 3 M KCl capped with a Vycor tip. The counter electrode was a platinum wire. All electrolyte solutions were purged for a minimum of 20 min in Ar prior to the measurements, and a blanket of Ar was maintained over the solutions during the measurements. All solutions except for D_2O experiments were prepared using deionized Millipore water (18.2 MΩ·cm) obtained from a Milli-Q water system. All experiments were conducted at room temperature (21 ± 1 °C).

Chronoamperometric (CA) Experiments. All CA experiments were run under the same solution and electrode conditions as CV experiments described above. A CHInstruments 660B potentiostat was used to apply the square wave potential. The potentials were stepped from 0 to 0.8 V vs Ag/AgCl for 10 square wave cycles. Different overpotential values were obtained by changing the step height of the square wave, which always began at 0 V to ensure the monolayer was completely in its reduced form. The 10 resulting $i-t$ responses were sum-averaged into one average response. The final averaged $i-t$ curves were analyzed using OriginLab 7.0 software.

Results and Discussion

Synthesis and Characterization. The synthesis of the ferrocenoyl-diprolinyl-glycyl-cystamines $[Fc\text{-}(Pro_2\text{-}Gly)_n\text{-}CSA]_2$ ($n = 1-3$; **1**−**3**) was carried out in an stepwise fashion analogous to the synthesis reported for the Fc-oligoprolinyl-cystamine conjugates,[20] starting from cystamine dihydrochloride ($[CSA]_2$·2HCl) and Boc-Pro_2Gly-OH. The three Fc-peptide conjugates **1**−**3** were obtained as yellow to orange solids and were characterized by spectroscopic techniques. The NMR characteristics compare well with other monosubstituted Fc-peptides.[51−57] Addition of D_2O to chloroform solutions of the Fc-peptides **1**−**3** causes exchange of the amide protons, as clearly shown by ^{1}H NMR experiments (see Supporting Information). Rapid amide proton exchange points to the presence of several interchanging H-bonded and non-H-bonded populations in solution.[58−62]

In the IR spectrum, all compounds display strong amide I absorptions in the solid state and in solution. The N−H stretching region shows multiple signals indicating the involvement of the peptides in H-bonding, as would be expected for these systems. The nature of this interaction was investigated further by variable temperature circular dichroism (VT-CD) spectroscopy in EtOH. We chose EtOH as solvent because this solvent is used to deposit the Fc-peptide-cystamines onto gold. The CD spectra together with the melting curve collected at 209 nm of conjugates **1**−**3** are shown in Figure 2. There are some noticeable differences between compound **1** and compounds **2** and **3**. Fc-peptides **2** and **3** exhibit a strong negative ellipticity at 209 nm comparable to that exhibited by collagens, and thus we conclude that **2** and **3** adopt collagen-like helices. Furthermore, both show clear melting temperatures of 43 (2) °C and 52 (2) °C for **2** and **3**, respectively. Expectedly, Fc-peptide **1** does not form a collagen-like structure in EtOH, as indicated by the profile of the CD spectrum, due to its shorter length, and exists presumably mainly as the monomer, which is able to engage in H-bonding to adjacent molecules. UV−vis spectroscopy shows little difference in λ_{max} values (440 nm), indicating no electronic effects were induced on the Fc by increasing the pondant chain length. Next, we investigated the

TABLE 1: Solution Properties for Compounds 1−3[a]

compd	λ/nm	ϵ/M^{-1} cm^{-1}	$E_{1/2}$/mV	ΔE/mV	I_o/I_R	$D_0 \times 10^5$/cm·s^{-1}
1	443 (0.4)	550 (4)	570 (3)	66	1.06	1.2 (0.2)
2	438 (0.8)	470 (7)	556 (2)	64	1.05	2.4 (0.1)
3	444 (0.4)	420 (6)	553 (3)	61	1.03	5.0 (0.1)

[a] UV−vis measurements were carried out at 0.1 mM concentrations in acetonitrile. Solution electrochemistry of 1 mM Fc-peptides **1**−**3** in 0.1 M TBAP/CH_3CN at a scan rate of 100 mV·s^{-1} using glassy carbon electrode (BAS, 7.1 × 10^{-2} cm^2), Pt wire counter electrode, and Ag/AgCl reference electrode.

TABLE 2: RAIRS of Amide Bands of Fc-peptides 1−3

film	amide I/cm^{-1}	amide II/cm^{-1}	amide NH/cm^{-1}	amide I/amide II
1	1612	1545	3122, 3502	1.45
2	1613	1543	3123, 3502	1.58
3	1613	1545	3165, 3501	1.63

electrochemical properties of compounds **1**−**3** in acetonitrile solution. All compounds exhibit a fully reversible Fc-based one-electron oxidation, as judged from the peak separation and the ratio of peak currents. Table 1 summarizes the electrochemical properties of compounds **1**−**3**. The half-wave potential, $E_{1/2}$, values for compounds **2** and **3** are slightly lower than that of compound **1**. Similar changes in the redox potentials were observed in the series of Fc-oligoproline benzyl esters[57] and more recently in Aib-rich peptides.[35]

Film Preparations and Characterizations. Films of Fc-peptides **1**−**3** were prepared by incubating gold substrates in a deoxygenated 1 mM ethanolic solution of the Fc-peptide-cystamine conjugate for 5 days to ensure well-formed peptide films. After removal of unspecifically bound peptide by sonication, the modified gold surfaces were incubated in a deoxygenated 1 mM ethanolic solution of hexanethiol for 10 min. The net result of this step is the dilution of the electroactive Fc-peptide films by the hexanethiol.

The structure of the peptide films was investigated by various methods, including reflection absorption infrared spectroscopy (RAIRS), ellipsometry, and electrochemical methods. Using RAIRS, we measured the intensity of the amide I and II bands (Table 2) and we determined the angle of the Fc-peptide conjugate with respect to the surface normal from the ratio of amide I to II (Supporting Information).[20] The film thickness was determined by ellipsometry. The experimental results of the RAIRS study of Fc-conjugates **1**−**3** are summarized in Table 2. In addition, two N−H stretches were observed, clearly indicating the presence of H-bonded peptides on the surface. The surface angles and film thicknesses for peptides **1**−**3** are summarized in Table 3. The film tilt angle for Fc-peptides **1**−**3** is between 50° and 55°, which indicates that the packing behavior of the peptides is similar. Films formed from the Au−S spontaneous chemisorption process are generally formed at an angle to the Au surface. Very few films exhibit 0° deviation from surface normal. Several parameters determine the film tilt angle including the metal interface, the chemisorption species, and the intermolecular interactions such as van der Waals and dipole−dipole. As expected, film thickness increases concomitantly with the Fc-peptide conjugate length.

Electrochemical Studies. CV of films of compound **3** on 50 μm gold electrodes is shown in Figure 3. All surface CV experiments were carried out in H_2O and D_2O in the presence of 2 M $NaClO_4$ as supporting electrolyte in order to minimize the *iR* drop.

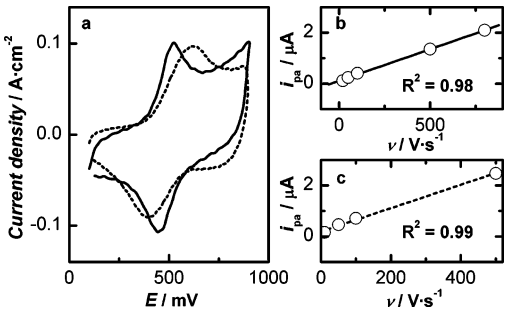

Figure 3. (a) CVs of a film of the Fc-peptide **3** on gold in H_2O (—) and D_2O (---) at a scan rate of 500 V·s^{-1} in 2 M $NaClO_4$, Pt counter electrode vs Ag/AgCl reference. Linear relationship between scan rate and anodic peak current for H_2O (b) and D_2O (c).

Integration of the faradaic peak currents of the CV curves allows us to evaluate the surface concentration of Fc-peptide-cystamine conjugates covalently linked to the surface by an Au−S linkage. Upon chemisorption of the Fc-peptide-cystamine, it is envisioned that the disulfide bond is cleaved to give gold−thiolate linkages as was reported before.[63] The peak current from the CVs increases linearly with scan rate, shown in Figure 3b,c, as is expected for an adsorbed film.[64] The $E^{\circ\prime}$ of the hexanethiol-diluted peptide self-assembled monolayer (SAM) decreases slightly as the Fc group is positioned further from the surface, as shown in Table 3. This may be rationalized in terms of the increase in the number of intermolecular H-bonds that occurs with the extension of the peptide chain. A similar H-bonding effect was observed by Maran[35] for Aib-peptides pointing toward the importance of H-bonding in relaying electronic information.

The integration of the background-subtracted anodic peak current of the CVs provides Fc-based surface coverage values of the mixed film in the range of 2.6 × 10^{-11}−1.0 × 10^{-11} mol·cm^{-2}, thus showing that exposure of the peptide film to a solution of hexanethiol causes dilution of the Fc-peptide. Table 3 summarizes the coverage obtained for undiluted and diluted Fc-peptide films. The overall decrease in peptide coverage is approximately 25%. This dilution step serves the purpose of filling pinholes and separating the Fc groups to minimize lateral interactions between electroactive groups, which may influence the ET kinetics. A 25% decrease in Fc concentration is typical[65] when considering peptidic systems under the conditions used in this paper to dilute monolayers. The replacement of 25% of

TABLE 3: Surface Characterization of Hexanethiol-Diluted SAMs of Fc-peptides 1−3 Bound to Au Surfaces[a]

				Γ/mol·cm^{-2}	
	$E^{\circ\prime}$ (mV)	angle[b] (deg)	thickness[c] (Å)	concentrated	diluted
1	480 (15)	50 (3)	12 (1)	3.4 (0.3) × 10^{-11}	2.6 (0.3) × 10^{-11}
2	460 (15)	55 (4)	16 (2)	3.0 (0.3) × 10^{-11}	2.0 (0.3) × 10^{-11}
3	454 (8)	55 (3)	22 (2)	1.0 (0.2) × 10^{-11}	7.5 (0.3) × 10^{-12}

[a] 2 M $NaClO_4$, Ag/AgCl reference. [b] Angles from surface normal. [c] Thickness measured by ellipsometry.

TABLE 4: Circuit Parameters from EIS Data for Hexanethiol-Mixed Films of Fc-peptides 1−3 in 2 M $NaClO_4$ in H_2O[a]

		Q_{dl}			
compd	R_S/Ω	$Y_o \times 10^{-6}/\Omega^{-1}\ s^n$	$n \pm 0.05$	$R_{CT} \times 10^4/\Omega$	$W \times 10^{-6}/\Omega^{-1}\ s^{1/2}$
1	55 (5)	1.5 (0.3)	0.9	4.2 (0.2)	1.4 (0.2)
2	52 (7)	0.6 (0.4)	0.9	6.3 (0.2)	1.3 (0.3)
3	151 (10)	1.0 (0.2)	0.9	8.5 (0.1)	2.2 (0.5)

[a] Values in parentheses represent standard deviations calculated from five films, not the errors from curve fitting.

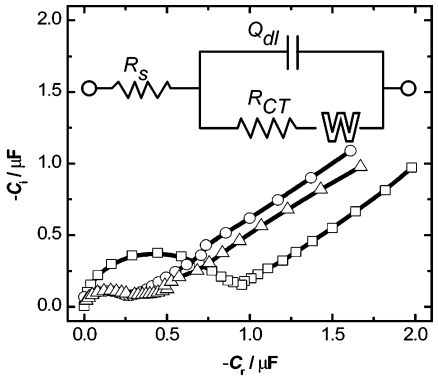

Figure 4. Impedance data for **1**−**3**. Equivalent circuits for fitting hexanethiol-diluted Fc-peptide-cystamine films. R_S = solution resistance; Q_{dl} = CPE of double-layer capacitance; R_{CT} = charge-transfer resistance; W = Warburg diffusion element. EIS data for diluted Fc-peptides **1** (○), **2** (△); and **3** (□) in the complex capacitance plane (at an applied bias voltage of $E^{\circ\prime}$ vs Ag/AgCl for the Fc group and ac amplitude of 5 mV rms in 2 M $NaClO_4$ at room temperature (from 100 kHz to 1 Hz).

the Fc-peptides in 10 min is expected because of the high affinity that the thiol has for the Au and peptides are known to pack loosely on the surface, predisposing them to replacement.

To evaluate the electronic characteristics of the Fc-peptide-cystamine SAM in more detail, we carried out electrochemical impedance spectroscopy (EIS) experiments in which the applied potential was the $E^{\circ\prime}$ of the Fc moiety. EIS is commonly interpreted with the help of equivalence circuits. The films are analyzed in terms of electronic circuit components, such as resistors and capacitors, which are related to the molecular characteristics of the film. The impedance spectra, acquired at 31 frequencies ranging from 0.1 Hz to 100 kHz at an applied potential equivalent to the $E^{\circ\prime}$ of the individual Fc-peptide conjugate, are shown in Figure 4. We fit all spectra to the same equivalent circuit shown as the inset of Figure 4, which includes a mass transport term as a Warburg variable impedance element. The inclusion of a mass transport circuit element was unexpected considering the Fc moiety was surface bound and diffusion effects are expected to be negligible.[66] Since all EIS experiments were run at an applied potential corresponding to the $E^{\circ\prime}$ value of the Fc group, the inclusion of a diffusion element in the equivalent circuit model implies that diffusion occurs concurrent with electron transfer. Table 4 shows the circuit element values obtained for films of Fc-peptides **1**−**3** on Au surfaces.

The solution resistance, R_S, for all compounds remains unchanged in H_2O and D_2O, which is expected since all films were analyzed at the same ionic strength of the electrolyte. The constant phase element (CPE), Q_{dl}, describes the double-layer pseudocapacitance and is used to account for the inhomogeneity of the film due to surface roughness effects. It is termed "pseudocapacitance" because the additional exponential modifier term, n, would have a value of 1 if it was a perfect capacitor.[67] Capacitance is inversely proportional to monolayer thickness, and the expected trend of decreasing Q_{dl} with increasing spacer length was observed. In all cases, the exponential factor was close to unity. R_{CT} is the resistance to charge transfer, which is one component necessary for the electron-transfer rate constant calculation. As the film thickness increases with increasing length of the peptide, R_{CT} increases. The Warburg diffusion element W increases as the peptide spacer increases in length.

ET kinetics for the mixed Fc-peptide/hexanethiol film were evaluated by CV[65] and CA.[68] Both methods gave comparable k_{ET}'s. k_{ET} values decrease as a function of the peptide length.[14] In the case of compound **1**, a film thickness of 12 (1) Å was obtained ellipsometrically and a k_{ET} of 10.9 (2.3) $\times$ 10^3 s^{-1} was measured in H_2O. Importantly, k_{ET} decreased to 7.3 (1.2) $\times$ 10^3 s^{-1} when the measurements were carried out in D_2O. k_{H_2O}/k_{D_2O} for compound **1** was 1.5. For compound **2**, the ratio k_{H_2O}/k_{D_2O} was 1.1, and for compound **3**, a ratio k_{H_2O}/k_{D_2O} of 1.2 was observed. Although the differences between H_2O and D_2O are small, these differences are reproducible and significant. Small kinetic isotope effects (KIEs) were observed before in unrelated biological systems. For example, Shafirovich et al. reported the KIE for an ET reaction involving DNA duplexes.[26] The k_{H_2O}/k_{D_2O} for this reaction ranged from 1.3 to 1.7. Thorp and co-workers also measured the ET rates from guanine to Ru complexes and reported a ratio k_{H_2O}/k_{D_2O} for this reaction of 2.[69] Kinetic measurements of the same author using different metal centers produce significantly higher kinetic isotope effects ranging from about 2.7 to 10.[70] Faver and co-workers studied the intramolecular electron transfer of azurin in H_2O and D_2O over a broad temperature range and found a kinetic deuterium isotope effect, k_H/k_D, which is *smaller* than unity (0.7 at 298 K).[71] A recent experimental study by Morita and Kimura[11] on electron-transfer properties claim that the ET process involves inelastic hopping of electrons between amide groups. However, the authors of this study did not provide any results of kinetic isotope effects. A comparison between a film prepared from $[Fc\text{-}Pro_6\text{-}CSA]_2$ and a system of similar length $[Fc\text{-}(Pro_2Gly)_2\text{-}CSA]_2$ may be instructive. In both cases, the film thickness is about 16 (2) Å. The number of the amino acid residues is identical. However, for $[Fc\text{-}Pro_6\text{-}CSA]_2$ the k_{ET} is 1.8 $\times$ 10^3 s^{-1}, whereas for $[Fc\text{-}(Pro_2Gly)_2\text{-}CSA]_2$ the k_{ET} is 6.6 $\times$ 10^3 s^{-1}. Structurally the two systems are related. The fundamental chemical difference is the inherent ability of $[Fc\text{-}(Pro_2Gly)_2\text{-}CSA]_2$ to engage in C═O···H−N H-bonding, which is not possible for oligoprolines. RAIRS spectra have confirmed the presence of H-bonding in the film. From our NMR studies, we know that the amide NH fully exchanges for deuterons in the presence of D_2O (see Supporting Information). The ET kinetics of a peptide in which the amide NHs were exchanged to NDs prior to film formation are identical to those in which H/D exchange takes place on the surface. $E^{\circ\prime}$, ΔE, and i_o/i_R were not affected by the change of H_2O to D_2O, suggesting that differential solvation of the N-terminal Fc headgroup is not the dominant factor.

We suggest the following explanation for our observations: Given the difference between the solution structures of compound **1** on one hand and compounds **2** and **3** on the other hand, it is unlikely that the surface structures are the same. However,

in all three cases, we observed a difference between $k_{ET}(H_2O)$ and $k_{ET}(D_2O)$, regardless of potential structural differences among the three peptide films (e.g., formation of specific surface aggregates). To rationalize the isotope effect on k_{ET}, we suggest the involvement of H-bonding in the ET process. Furthermore, k_{ET} exhibits shallow distance dependence. This suggests that through-space tunneling is not the major ET pathway, as significantly higher distance dependence would be expected (ca. 1 order of magnitude per 2.3 Å).

To calculate the exponential tunneling rates, eq 1, following Kimura,[11] was used.

$$k_{ET} = k_{ET}^{0} \exp(-\beta_A n_A - \beta_B n_B - \beta_C d_C) \qquad (1)$$

where k_{ET}^0, β_A, and β_B are the preexponential factor, the tunneling constants per carbon atom number for the cystamine CH_2 groups, and the cystamine amide group which are taken to be 3×10^8 s^{-1}, 1.2 and 0.5, respectively. According to Kimura[11] the tunneling constant, β_C, per length for a helical peptide chain is 6.6 nm^{-1}. The atom numbers involved in the methylene chain and amide group n_A and n_B are taken to be 2 and 1, respectively. The sulfur atom and amide group involved in the ferrocene tether were omitted since the lengths of the Au−S and N−C bonds are approximately the same as the distance between a free ferrocene in solution and an electrode at the closest approach, as described in the literature.[19] The chain lengths, d_C, of **1**, **2**, and **3** were 12, 16, and 28 Å, respectively. Peptide lengths were calculated from crystallographic dimensions ((8.0 Å)[PPG repeat]$^{-1}$) and an energy-minimized CSA fragment distance (4.0 Å, Chem 3D) and resulted in k_{ET}'s of 6000, 31, and 0.2 s^{-1} for **1**, **2**, and **3**, respectively. It is clear from the calculated k_{ET} values that peptides **2** and **3** do not follow a superexchange mechanism, whereas peptide **1** could operate under this mechanism.

Theoretical work that accounts for both tunneling and friction controlled charge-transfer mechanisms and the transition zone between the two mechanisms is available.[9,14−16,72−76] An adaptation of the unified expression for rate constants at electrode surfaces has been realized by Waldeck,[77] wherein the crossover from adiabatic (strong coupling, friction control) to nonadiabatic (weak coupling, tunneling) regimes is described in detail. ET in a structured medium with large relaxation times and small reorganizational energies (i.e., proteins) exhibit transitions between adiabatic and nonadiabatic mechanisms that occur at small electronic coupling factor magnitudes and result in long-distance charge transfer. It is possible that our peptides span that transition from nonadiabatic (peptide **1**) to adiabatic charge transfer (peptides **2** and **3**) and remain under frictional control. This mechanistic interpretation can account for the experimentally observed rate of 4.2 (1.2) $\times 10^3$ s^{-1}, which is 4 orders of magnitude larger than the calculated rate constant if the peptide were operating under a superexchange mechanism.[11] Assuming an adiabatically controlled system for **2** and **3**, the frictional component can arise from the conformational motion of the peptide upon oxidation and reduction. Conformational motion of "catalytic water" is known to contribute to frictional coupling, and the D_2O results are consistent with the ET reaction involving water(s) bound to the peptide.[77]

Jortner and co-workers showed that while a short-range two-center one-step superexchange charge transfer follows an exponential relationship, a multistep resonance charge transport results in a weak algebraic distance dependence.[78] The crossover between one-step superexchange mediated charge transfer and multistep thermally induced hopping (TIH) occurs at a "critical" value of the bridge size. k_{ET} is influenced by the energy gap between donor and acceptor, the nearest-neighbor electronic couplings, and the temperature.[79] As the temperature increases, k_{ET} is expected to increase. Figure 5 shows a summary of the k_{ET}'s for peptides **1**−**3** and of other related Fc-amino acid and Fc-peptide conjugates $[Fc\text{-}Gly\text{-}CSA]_2$, $[Fc\text{-}Ala\text{-}CSA]_2$, $[Fc\text{-}Ala_2\text{-}CSA]_2$, and $[Fc\text{-}Phe\text{-}Ala\text{-}CSA]_2$, and the series of $[Fc\text{-}Pro_n\text{-}CSA]_2$ ($n = 0-6$). For the shorter conjugates $[Fc\text{-}Gly\text{-}CSA]_2$, $[Fc\text{-}Ala\text{-}CSA]_2$, $[Fc\text{-}Ala_2\text{-}CSA]_2$, and $[Fc\text{-}Phe\text{-}Ala\text{-}CSA]_2$, the film thicknesses range from 6 (1) to 9 (1) Å and k_{ET}'s are between 5.3×10^3 and 7.8×10^3 s^{-1}.[65] For the $[Fc\text{-}Pro_n\text{-}CSA]_2$ series, k_{ET} ranges from 1.8×10^3 to 11.2×10^3 s^{-1}.[20] We make two observations: (a) for very short peptides, k_{ET}'s are virtually independent of film thickness, and (b) a linear relationship between the length of the peptide spacer and k_{ET} was observed. Similar experimental results were obtained by Waldeck, Niki, and Bowden, who showed that for short alkyl spacers the k_{ET}'s are independent of distance but do not follow the simple nonadiabatic ET kinetics.[77,80−84]

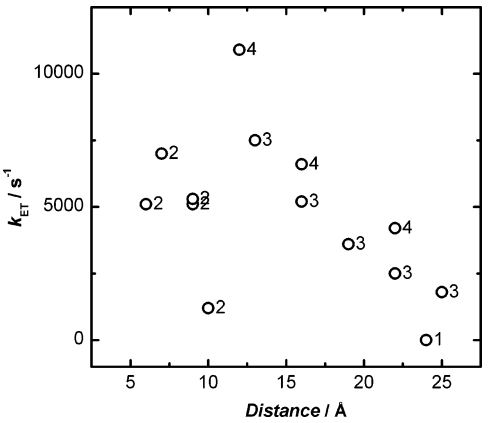

Figure 5. Comparison of ET rate constants obtained from several Fc-labeled peptide films. Points labeled 1,[11] 2,[65] and 3[20] are taken from the indicated references, and points labeled 4 are from this work.

Figure 5 shows a compilation of ET kinetic results from several papers plotted as a function of the peptide spacer length. The decrease in k_{ET} is not exponential and has a large variance, implying that peptide spacers >5 Å do not undergo electron tunneling and that the degree of H-bonding may play an important role in ET reactions.

Important in this regard is also that the solvent and temperature influence the rate of the ET reaction, as was shown by Bixon and Jortner.[79]

Variable-Temperature Studies. We carried out variable-temperature (VT) impedance studies to gain further insight into the role of the H-bonded interface in the electron-transfer process. Impedance spectra were recorded at temperatures between 7 and 30 °C, where covalent bonds within the peptides and the Au−S interactions are known to be stable.[85−87] An additional 10 min period was taken once the set temperature was reached before the EIS was recorded to allow for equilibrium conditions. The EIS curves were fit to the same equivalent circuit shown in Figure 5, and the resulting circuit element values are shown in Table 5. Monolayers are known to rearrange on the surface by an increase in temperature. However, the purpose of the VT study was to perturb the H-bonding network and measure the result in terms of changes in equivalent circuit parameters. Thus, surface reorganization was not investigated in detail at this stage, but current experiments involving VT imaging experiments are underway to investigate the structural hysteresis upon heating and subsequent cooling.

TABLE 5: Circuit Parameters from EIS Data for Hexanethiol-Mixed Films of Fc-peptides 1−3 in 2 M $NaClO_4$ in H_2O at Various Solution Temperatures

			Q_{dl}			
compd	temp/°C	$R_S \pm 5/\Omega$	$Y_o \times 10^{-6}/\Omega^{-1}$ s^n	$n \pm 0.05$	$R_{CT} \times 10^4/\Omega$	$W \times 10^{-6}/\Omega^{-1}$ s$^{1/2}$
1	7.7	69	2.3	0.8	15.1	0.4
	11.9	59	2.0	0.9	7.7	0.8
	18.9	56	1.8	0.9	5.3	1.1
	24.7	55	1.5	0.9	4.2	1.4
	30	73	1.0	0.9	1.4	1.8
2	7.1	65	1.0	0.9	17.3	0.8
	14.4	57	0.8	0.9	12.7	1.1
	19.1	62	0.6	0.9	6.3	1.3
3	8.4	95	1.4	0.9	22.8	1.5
	11.8	104	1.3	0.9	14.9	1.8
	17.4	93	1.2	0.9	9.3	2.0
	23.7	152	1.1	0.9	8.5	2.2

Above we described that, in order to model the impedance spectra recorded at the $E^{\circ\prime}$, it was necessary to include a diffusion element. This diffusion element accounts for the movement of the Fc-peptide as it responds to different electric field strengths in its reduced and oxidized forms. Upon oxidation, the positively charged Fc group will be repelled from the positive electrode surface (see Figure 6a). This rearrangement is expected to cause the reorientation of dipoles or weakening of some of the interpeptide H-bonds. Alternatively, as shown by Figure 6b, the oxidation of the N-terminal Fc headgroup on each of the peptides will cause electrostatic repulsion between each Fc in the peptide chain, resulting in weakening of the interpeptide H-bonding. Both models are supported by the inclusion of a Warburg diffusion element in the modeling of the impedance data. Furthermore, these results support an ET mechanism that is under frictional control. For Fc-DNA films, oxidation of the Fc group causes significant motion within the film, which was recently analyzed.[88] The observed isotope effect is not likely due to different solvation energies because Fc redox is very sensitive to solvent effects[89] and the $E^{\circ\prime}$ values in H_2O and D_2O are identical. However, the solvent reorganization immediately surrounding the Fc when it is oxidized or reduced could also contribute to the observed isotope effect. Despite an unclear mechanism, this work is further evidence that H-bonding plays a key role in ET through peptide films.

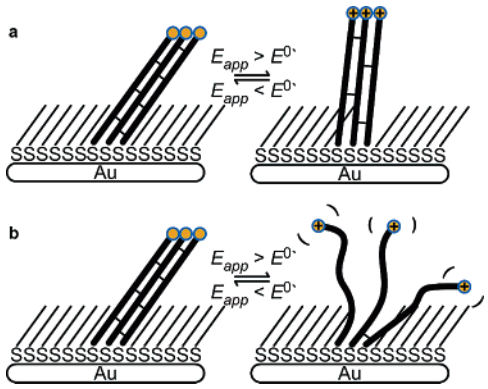

Figure 6. Schematic of the H-bonded assembly in response to an applied potential. (a) The oxidation of the Fc group forces the shearing of some of the H-bonds because the Fc^+ is electrostatically pushed away from the positive bias placed on the electrode. (b) The oxidation of the Fc to Fc^+ produces enough electrostatic repulsion to drive the Fc^+ headgroups away from one another, resulting in the fraying of some of the H-bonds at the top of the film.

Conclusion

The synthesis and characterization of a series of Fc- and CSA-peptides were carried out. The tripeptide repeat sequence, Pro-Pro-Gly, was used because of its structural parallels to natural collagen. CD studies suggest significant differences in the structure of the Fc-labeled peptide assemblies. However, the longest member of the series adopts the desired triple helical structure in solution. Films of the peptides were formed on Au electrodes and characterized by RAIRS, ellipsometry, and electrochemistry. The film thickness increases with the length of the peptide spacer and the Fc-peptides are H-bonded on the surface. From our electrochemical measurements (CV and CA) in H_2O and D_2O, the ET kinetics were obtained, which show a linear and shallow dependence of k_{ET} on film thickness. ET studies in D_2O show that the ET rates are slower and a KIE of 1.2−1.6 was observed. Our experimental findings suggest electron transfer from the Fc headgroup to the Au surface via the peptide spacer, presumably following Jortner's TIH mechanism. It is tempting to point to a recent proposal of electron hopping from amide to amide in peptides,[11] and to further suggest electron entrainment in the H-bonded Fc-peptide conjugate. In our experiments, the time scale of the electron movement from the Fc to the gold surface in compounds **1**−**3** is on the millisecond time scale, which is slower than the movement of small functional groups.[90,91] Thus, we speculate that movement of the entire molecule (e.g., breathing motions of the H-bonding network, rocking motion of the individual peptide strands) may be responsible for the isotope effect. It was shown by several groups that the nuclear dynamics contributes to the ET rate significantly.[92,93] Similarly, Onuchic and co-workers[94] have demonstrated the influence of H-bonds in azurin using molecular dynamics calculations (MD). In the Fc-peptide conjugates described here, we can assume that MD is playing an important role in determining the exact mechanistic pathway. However, in the absence of detailed molecular dynamics calculations, this remains an open and unanswered question.

Acknowledgment. The authors thank NSERC for funding. H.-B.K. is the Canada Research Chair in Biomaterials.

Supporting Information Available: ^{1}H NMR amide H/D exchange data, solution CVs of Fc-peptides, surface FT-IR and KBr disk, CV data of concentrated vs mixed films of Fc-peptides, CA results for **3** in D_2O and H_2O (PDF). This material is available free of charge via the Internet at http://pubs.acs.org.

References and Notes

(1) Bobrowski, K.; Poznanski, J.; Holcman, J.; Wierzchowski, K. L. *J. Phys. Chem. B* **1999**, *103*, 10316−10324.

(2) DeFelippis, M. R.; Faraggi, M.; Klapper, M. H. *J. Am. Chem. Soc.* **1990**, *112*, 5640−5642.
(3) Farver, O.; Pecht, I. *J. Biol. Inorg. Chem.* **1997**, *2*, 387−392.
(4) Gray, H. B.; Winkler, J. R. *Annu. Rev. Biochem.* **1996**, *65*, 537−561.
(5) Gray, H. B.; Winkler, J. R. *J. Electroanal. Chem.* **1997**, *438*, 43−47.
(6) Isied, S. S.; Ogawa, M. Y.; Wishart, J. F. *Chem. Rev.* **1992**, *92*, 381−394.
(7) Koch, T.; Armitage, B.; Hansen, H. F.; Orum, H.; Schuster, G. B. *Nucleosides Nucleotides* **1999**, *18*, 1313−1315.
(8) Lang, K.; Kuki, A. *Photochem. Photobiol.* **1999**, *70*, 579−584.
(9) Langen, R.; Chang, I. J.; Germanas, J. P.; Richards, J. H.; Winkler, J. R.; Gray, H. B. *Science* **1995**, *268*, 1733−1735.
(10) Langen, R.; Colon, J. L.; Casimiro, D. R.; Karpishin, T. B.; Winkler, J. R.; Gray, H. B. *J. Biol. Inorg. Chem.* **1996**, *1*, 221−225.
(11) Morita, T.; Kimura, S. *J. Am. Chem. Soc.* **2003**, *125*, 8732−8733.
(12) Ogawa, M. Y.; Moreira, I.; Wishart, J. F.; Isied, S. S. *Chem. Phys.* **1993**, *176*, 589−600.
(13) Petrov, E. G.; Shevchenko, Y. V.; May, V. *Chem. Phys.* **2003**, *288*, 269−279.
(14) Petrov, E. G.; Shevchenko, Y. V.; Teslenko, V. I.; May, V. *J. Chem. Phys.* **2001**, *115*, 7107−7122.
(15) Petrov, E. G.; Zelinskyy, Y. R.; May, V. *J. Phys. Chem. B* **2002**, *106*, 3092−3102.
(16) Winkler, J. R.; Di Bilio, A. J.; Farrow, N. A.; Richards, J. H.; Gray, H. B. *Pure Appl. Chem.* **1999**, *71*, 1753−1764.
(17) Winkler, J. R.; Gray, H. B. *Chem. Rev.* **1992**, *92*, 369−379.
(18) Zheng, Y. J.; Case, M. A.; Wishart, J. F.; McLendon, G. L. *J. Phys. Chem. B* **2003**, *107*, 7288−7292.
(19) Sisido, M.; Hoshino, S.; Kusano, H.; Kuragaki, M.; Makino, M.; Sasaki, H.; Smith, T. A.; Ghiggino, K. P. *J. Phys. Chem. B* **2001**, *105*, 10407−10415.
(20) Galka, M. M.; Kraatz, H. B. *ChemPhysChem* **2002**, *3*, 356−359.
(21) Isied, S. S.; Ogawa, M. Y.; Wishart, J. F. *Chem. Rev.* **1992**, *92*, 381−394.
(22) Williams, R. J. P. *J. Biol. Inorg. Chem.* **1997**, *2*, 373−377.
(23) Beratan, D. N.; Skourtis, S. S. *Curr. Opin. Chem. Biol.* **1998**, *2*, 235−243.
(24) Farver, O.; Kroneck, P. M. H.; Zumft, W. G.; Pecht, I. *J. Inorg. Biochem.* **2001**, *86*, 84−84.
(25) Scott, R. A. *J. Biol. Inorg. Chem.* **1997**, *2*, 372−372.
(26) Shafirovich, V.; Dourandin, A.; Geacintov, N. E. *J. Phys. Chem. B* **2001**, *105*, 8431−8435.
(27) Skourtis, S. S.; Beratan, D. N. *J. Biol. Inorg. Chem.* **1997**, *2*, 378−386.
(28) Skourtis, S. S.; Beratan, D. N. In *Electron Transfer—from Isolated Molecules to Biomolecules, Part 1*; John Wiley & Sons Inc.: New York, 1999; Vol. 106, pp 377−452.
(29) de Rege, P. J. F.; Williams, S. A.; Therien, M. J. *Science* **1995**, *269*, 1409−1413.
(30) Turro, C.; Chang, C. K.; Leroi, G. E.; Cukier, R. I.; Nocera, D. G. *J. Am. Chem. Soc.* **1992**, *114*, 4013−4015.
(31) Zaleski, J. M.; Turro, C.; Mussell, R. D.; Nocera, D. G. *Coord. Chem. Rev.* **1994**, *132*, 249−258.
(32) Roberts, J. A.; Kirby, J. P.; Nocera, D. G. *J. Am. Chem. Soc.* **1995**, *117*, 8051−8052.
(33) Kirby, J. P.; Vandantzig, N. A.; Chang, C. K.; Nocera, D. G. *Tetrahedron Lett.* **1995**, *36*, 3477−3480.
(34) Tecilla, P.; Dixon, R. P.; Slobodkin, G.; Alavi, D. S.; Waldeck, D. H.; Hamilton, A. D. *J. Am. Chem. Soc.* **1990**, *112*, 9408−9410.
(35) Antonello, S.; Formaggio, F.; Moretto, A.; Toniolo, C.; Maran, F. *J. Am. Chem. Soc.* **2003**, *125*, 2874−2875.
(36) (a) Sek, S.; Moszynski, R.; Sepiol, A.; Misicka, A.; Bilewicz, R. *J. Electroanal. Chem.* **2003**, *550−551*, 359−364. (b) Sek, S.; Sepiol, A.; Tolak, A.; Misicka, A.; Bilewicz, R. *J. Phys. Chem. B* **2004**, *108*, 8102−8105
(37) Weber, K. S.; Creager, S. E. *J. Electroanal. Chem.* **1998**, *458*, 17−22.
(38) Chidsey, C. E. D. *Science* **1991**, *251*, 919−922.
(39) Finklea, H. O.; Hanshew, D. D. *J. Am. Chem. Soc.* **1992**, *114*, 3173−3181.
(40) Finklea, H. O.; Liu, L.; Ravenscroft, M. S.; Punturi, S. *J. Phys. Chem.* **1996**, *100*, 18852−18858.
(41) Bard, A. J.; Faulkner, L. R. *Electrochemical methods: fundamentals and applications*, 2nd ed.; John Wiley: New York, 2001.
(42) Ramachandran, G. N.; Kartha, G. *Nature* **1954**, *174*, 269−270.
(43) Ramachandran, G. N.; Kartha, G. *Nature* **1955**, *176*, 593−595.
(44) Rich, A.; Crick, F. H. *J. Mol. Biol.* **1961**, *3*, 483−506.
(45) Bretscher, L. E.; Jenkins, C. L.; Taylor, K. M.; DeRider, M. L.; Raines, R. T. *J. Am. Chem. Soc.* **2001**, *123*, 777−778.
(46) Fields, G. B. *Connect. Tissue Res.* **1995**, *31*, 235−243.
(47) Berg, R. A.; Olsen, B. R.; Prockop, D. J. *J. Biol. Chem.* **1970**, *245*, 5759−5763.
(48) Berg, R. A.; Prockop, D. J. *Biochem. Biophys. Res. Commun.* **1973**, *52*, 115−120.
(49) Mayo, K. H. *Biopolymers* **1996**, *40*, 359−370.
(50) Kramer, R. Z.; Vitagliano, L.; Bella, J.; Berisio, R.; Mazzarella, L.; Brodsky, B.; Zagari, A.; Berman, H. M. *J. Mol. Biol.* **1998**, *280*, 623.
(51) Moriuchi, T.; Yoshida, K.; Hirao, T. *Org. Lett.* **2003**, *5*, 4285−4288.
(52) Moriuchi, T.; Yoshida, K.; Hirao, T. *J. Organomet. Chem.* **2003**, *668*, 31−34.
(53) Moriuchi, T.; Nomoto, A.; Yoshida, K.; Ogawa, A.; Hirao, T. *J. Am. Chem. Soc.* **2001**, *123*, 68−75.
(54) Mandal, H. S.; Kraatz, H.-B. *J. Organomet. Chem.* **2003**, *674*, 32−37.
(55) Plumb, K.; Kraatz, H.-B. *Bioconjugate Chem.* **2003**, *14*, 601−606.
(56) Bediako-Amoa, I.; Silerova, R.; Kraatz, H.-B. *Chem. Commun.* **2002**, 2430−2431.
(57) Kraatz, H. B.; Leek, D. M.; Houmam, A.; Enright, G. D.; Lusztyk, J.; Wayner, D. D. M. *J. Organomet. Chem.* **1999**, *589*, 38−49.
(58) Roy, S.; Ratnaswamy, G.; Boice, J. A.; Fairman, R.; McLendon, G.; Hecht, M. H. *J. Am. Chem. Soc.* **1997**, *119*, 5302−5306.
(59) Jeng, M. F.; Englander, S. W.; Pardue, K.; Rogalskyj, J. S.; McLendon, G. *Nature Struct. Biol.* **1994**, *1*, 234−238.
(60) Connelly, G. P.; Bai, Y. W.; Jeng, M. F.; Englander, S. W. *Proteins: Struct., Funct., Genet.* **1993**, *17*, 87−92.
(61) Jeng, M. F.; Englander, S. W.; Elove, G. A.; Wand, A. J.; Roder, H. *Biochemistry* **1990**, *29*, 10433−10437.
(62) Hughson, F. M.; Wright, P. E.; Baldwin, R. L. *Science* **1990**, *249*, 1544−1548.
(63) Ishida, T.; Yamamoto, S. i.; Mizutani, W.; Motomatsu, M.; Tokumoto, H.; Hokari, H.; Azehara, H.; Fujihira, M. *Langmuir* **1997**, *13*, 3261−3265.
(64) Finklea, H. O. In *Electroanalytical Chemistry*; Bard, A. J., Rubinstein, I., Eds.; Marcel Dekker: New York, 1993; Vol. 19, pp 110−335.
(65) Bediako-Amoa, I.; Sutherland, T. C.; Li, C. Z.; Silerova, R.; Kraatz, H. B. *J. Phys. Chem. B* **2004**, *108*, 704−714.
(66) The Supporting Information contains the impedance spectrum of **3** that was fit to the circuit shown in Figure 4 without the Warburg diffusion element, and clearly, in the absence of a Warburg term, the fitting failed.
(67) Dijksma, M.; Boukamp, B. A.; Kamp, B.; van Bennekom, W. P. *Langmuir* **2002**, *8*, 3105−3112.
(68) Chronoamperometric experiments were run for **3** in D_2O and H_2O and yielded electron-transfer rate constants of 1.5×10^3 and 1.3×10^3 s^{-1}, respectively. Although the magnitudes of the rate constants are not the same as measured in CV, the kinetics isotope effect remains the same. However, the CA results showed large kinetic heterogeneity, which were apparent by the nonlinearity of the logarithmic plot of the current transients, and could have led to the difference in rate constant magnitudes. Thus, the accuracy of the rate constants determined by CA was suspect. It is possible that the observed kinetic heterogeneity could be due to the movement of the peptides under applied potentials, and CA kinetics models that account for diffusion of surface-confined redox probes are currently unavailable.
(69) Weatherly, S. C.; Yang, I. V.; Thorp, H. H. *J. Am. Chem. Soc.* **2001**, *123*, 1236−1237.
(70) Weatherly, S. C.; Yang, I. V.; Armistead, P. A.; Thorp, H. H. *J. Phys. Chem. B* **2003**, *107*, 372−378.
(71) Farver, O.; Zhang, J. D.; Chi, Q. J.; Pecht, I.; Ulstrup, J. *Proc. Natl. Acad. Sci. U.S.A.* **2001**, *98*, 4426−4430.
(72) Petrov, E. G.; May, V. *J. Phys. Chem. A* **2001**, *105*, 10176−10186.
(73) Sumi, H. *J. Electroanal. Chem.* **1997**, *438*, 11−20.
(74) Sumi, H.; Kakitani, T. *J. Phys. Chem. B* **2001**, *105*, 9603−9622.
(75) Onuchic, J. N.; Beratan, D. N.; Winkler, J. R.; Gray, H. B. *Annu. Rev. Biophys. Biomol. Struct.* **1992**, *21*, 349−377.
(76) Beratan, D. N.; Onuchic, J. N.; Winkler, J. R.; Gray, H. B. *Science* **1992**, *258*, 1740−1741.
(77) Khoshtariya, D. E.; Wei, J. J.; Liu, H. Y.; Yue, H. J.; Waldeck, D. H. *J. Am. Chem. Soc.* **2003**, *125*, 7704−7714.
(78) Jortner, J.; Bixon, M.; Langenbacher, T.; Michel-Beyerle, M. E. *Proc. Natl. Acad. Sci. U.S.A.* **1998**, *95*, 12759−12765.
(79) Bixon, M.; Jortner, J. *J. Am. Chem. Soc.* **2001**, *123*, 12556−12567.
(80) Avila, A.; Gregory, B. W.; Niki, K.; Cotton, T. M. *J. Phys. Chem. B* **2000**, *104*, 2759−2766.
(81) Feng, Z. Q.; Imabayashi, S.; Kakiuchi, T.; Niki, K. *J. Chem. Soc., Faraday Trans.* **1997**, *93*, 1367−1370.
(82) Song, S.; Clark, R. A.; Bowden, E. F.; Tarlov, M. J. *J. Phys. Chem.* **1993**, *97*, 6564−6572.
(83) Collinson, M.; Bowden, E. F.; Tarlov, M. J. *Langmuir* **1992**, *8*, 1247−1250.

(84) Tarlov, M. J.; Bowden, E. F. *J. Am. Chem. Soc.* **1991**, *113*, 1847−1849.

(85) Valiokas, R.; Oestblom, M.; Svedhem, S.; Svensson, S. C. T.; Liedberg, B. *J. Phys. Chem. B* **2002**, *106*, 10401−10409.

(86) Garg, N.; Carrasquillo-Molina, E.; Lee, T. R. *Langmuir* **2002**, *18*, 2717−2726.

(87) Ishida, T.; Fukushima, H.; Mizutani, W.; Miyashita, S.; Ogiso, H.; Ozaki, K.; Tokumoto, H. *Langmuir* **2002**, *18*, 83−92.

(88) Anne, A.; Bouchardon, A.; Moiroux, J. *J. Am. Chem. Soc.* **2003**, *125*, 1112−1113.

(89) Baker, M. V.; Kraatz, H. B.; Quail, J. W. *New J. Chem.* **2001**, *25*, 427−433.

(90) Spoerlein, S.; Carstens, H.; Satzger, H.; Renner, C.; Behrendt, R.; Morader, L.; Tavan, P.; Zinth, W.; Wachtveitl, J. *Proc. Natl. Acad. Sci. U.S.A.* **2002**, *99*, 7998−8002.

(91) Mayo, K. H.; Daragan, V. A.; Idiyatullin, D.; Nesmelova, I. *J. Magn. Reson.* **2000**, *146*, 188−195.

(92) Kawatsu, T.; Kakitani, T.; Yamato, T. *J. Phys. Chem. B* **2002**, *106*, 11356−11366.

(93) Kawatsu, T.; Kakitani, T.; Yamato, T. *J. Phys. Chem. B* **2002**, *106*, 5068−5074.

(94) Kobayashi, C.; Baldridge, K.; Onuchic, J. N. *J. Chem. Phys.* **2003**, *119*, 3550−3558.